Life Estimation of DC-Link Capacitor in Multi-operating Traction Drive System

Bo Yao[1], Xinglai Ge[1], Lingzhou Shu[2], Huimin Wang[1], Zilang Hu[1], and Bin Gou[3]
[1] Key Laboratory of Magnetic Suspension Technology and Maglev Vehicle, Ministry of Education, Southwest Jiaotong University, China
[2] School of Information and Software Engineering, University of Electronic Science and Technology of China, China
[3] the Rolls-Royce @ NTU Corporate Lab, Nanyang Technological University, Singapore

Abstract--**The reliability of DC-link capacitor in the traction drive system is regarded as a major problem that should be resolved well. Based on this, this paper proposes a life estimation method of DC-link capacitor to realize the reliability evaluation of the traction drive system. Starting from the capacitor life model, the actual multi-operating data is converted into the calculation of traction load through simulation tests, and the capacitor voltage and current ripple signals are obtained. Fourier method by combining the sliding window grouping with the neural network are used to analyze the dynamics of the hot spot temperature, and is optimized by use the Newton's law of cooling. Finally, the capacitor loss is analyzed through the experimental test results, and the safe operation of the system is considered, and the lifetime of the capacitor under multi-operating conditions is shown.**

Index Terms-- **DC-link capacitor, hot spot temperature, multi-operating conditions, traction drive system**

I. INTRODUCTION

Passive Components require extremely long operating cycles of more than a decade or even decades, which means that the lifetime and failure rate of the device should be carefully considered and designed at the beginning of the device layout.

The capacitor is considered as one of the most vulnerable components in power electronic systems, and the reliability of the capacitor increasingly becomes a concerning issue [1]. In high-speed traction drive system, the DC-link capacitor mainly plays the role of energy storage and filtering, so the reliability of DC-link capacitor is associated with the safety and the performance of high-speed traction drive system.

In recent years, the methods suited for the reliability of capacitors has been proposed in the shown literatures. In [2], the mathematical model of capacitor life is analyzed, and the failure determination of the capacitor is given. A method about the degradation of electrolytic capacitors in [3] is proposed, and the electro-thermal stress is related to the aging of capacitor. In [4], a lifetime estimation method of capacitor considering the influence of frequency and grid voltage unbalance is presented，and a long-term cumulative loss model of capacitance is established by a task profile based on a model of natural growth influence. The aging process of the capacitor and the equivalent resistance (ESR) is shown in [5], which is based on the life test results of the capacitor. A capacitor reliability evaluation method in the topology of the grid-connected diode rectifier circuit is proposed, and the nonlinear process of the ESR growth and capacitance reduction in the degradation process is considered in [6].

Performing a reasonable thermal analysis model is necessary to study the reliability of the capacitor. A more accurate calculation method of capacitance loss for aluminum electrolytic capacitors is discussed in [7]. A more accurate temperature and lifetime distribution is studied from the design stage in [8]. Models for estimating the hot spot temperature of a single capacitor more quickly are established in [9], [10]. At the same time, the traction drive system uses a series and parallel capacitor bank structure to obtain greater capacitance and voltage. An optimized capacitor bank design solution is discussed by building a model of convection and radiation heat transfer in [11]. A nonlinear mathematical model of capacitor banks based on thermal conduction, convection and radiation physics is proposed in [12], [13], and a simplified version of the model can also be demonstrated through the RC circuit network, which implements a more reasonable thermal stress modeling calculation.

In order to evaluate the reliability of the high-speed traction drive system, a lifetime estimation method is proposed in this paper. The implementation of the proposed method is starting from the capacitor life model. The actual multi-operating data is converted into the calculation of traction load through simulation test. The discrete Fourier method and the neural network are employed in the proposed method, and introduce Newton’s law of cooling to optimize the hot spot temperature. Meanwhile, the actual capacitance loss of the capacitor through the experimental test results is given. Finally, considering the safe multi-operating of the system, a reasonable evaluation of the lifetime of the DC-link capacitor is given.

II. LIFE MODEL AND MULTI-CASE SIMULATION TEST

A. DC-Link Capacitor Life Model

For aluminum electrolytic and film capacitors, the lifetime model is given as [1]:

$$L=L_0\times\left(\frac{V}{V_0}\right)^{-n}\times 2^{\frac{T_0-T_h}{p}} \tag{1}$$

where L and L_0 denote the actual lifetime and rated lifetime, V and V_0 denote the actual capacitor voltage and rated capacitor voltage, T_0 and T_h denote the rated temperature and actual hot spot temperature, n and p represent two empirical coefficients, respectively.

According to (1), the hot spot temperature is obtained as [3]:

$$T_h = T_a + R_{ha} \times \sum_{i=1}^{n} \left[ESR(f_i) \times I_{rms}^2(f_i) \right] \tag{2}$$

where $ESR(f_i)$ and $I_{rms}(f_i)$ represent the ESR and the root mean square(RMS) value of the ripple current at frequency f_i. T_a and R_{ha} are the ambient temperature and the equivalent thermal resistance.

B. AC-DC-AC Traction Drive System and Multi-Operating Conditions Test

A typical high-speed AC-DC-AC train traction drive system is shown in Fig.1. It consists of two parallel rectifiers, an intermediate DC bus, an inverter and an asynchronous motor. In order to improve the transmission efficiency, a lower switching frequency (450Hz) is set, so the large capacitance of the DC-link capacitor for energy storage and filtering in the system to ensure the stability of operation. The main parameters of the traction drive system are shown in Table I.

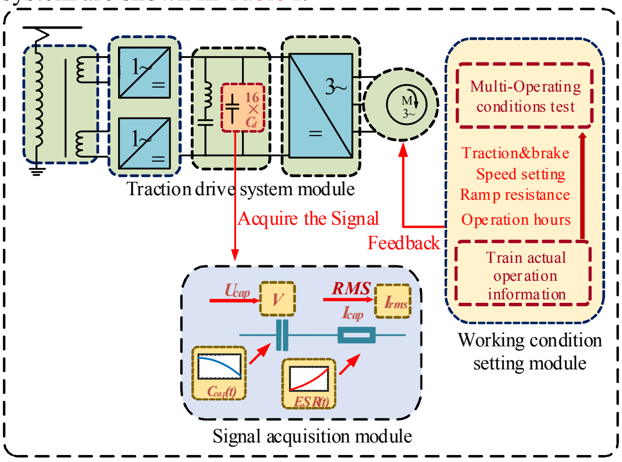

Fig. 1: The block diagram of a typical traction system

TABLE I
PARAMETERS OF THE TRACTION DRIVE SYSTEM

parameter	value	parameter	value
Grid side voltage	1550V	Motor rated power	562kV•A
Grid side frequency	50Hz	Motor frequency	135Hz
DC-link capacitance/ ESR	3.3mF/0.6mΩ	Filter inductor/capacitor	0.83mH /3mF
Switching frequency	450Hz	DC-Link voltage	3000V
Grid side leakage inductance	2.3mH	Grid side leakage resistance	0.2Ω

In the traction drive system, the basic gross resistance can be obtained according to the actual train running speed. At the same time, the additional gross resistance of the train can be obtained according to the actual altitude change and the curve of radius. These are finally fed back to the motor load, as shown in Fig.2.

The actual train speed, slope, time and other data, as shown in Table 2, are converted into traction load and gross resistance. The data are further converted to the traction drive system to simulate actual operating conditions.

TABLE II
MULTI-OPERATING CONDITION SETTING PARAMETERS

Driving range	Run/stop time (s)	Max speed (km/h)	Average slope
A→B	1980.1/120.1	249.89	0.2603
B→C	2158.9/180.0	286.30	0.2804
…	…	…	…
R→M	2469.1/180.2	269.45	-0.2362
M→N	3419.1/0	240.23	-0.3088

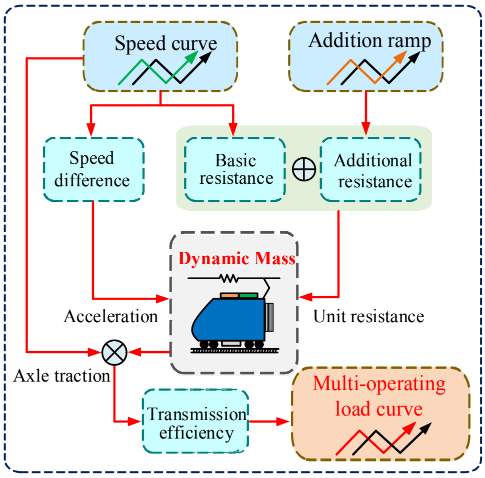

Fig. 2: The block diagram of multi-operating load calculation

C. DC-Link Capacitor Signal Acquisition

In the traction drive system, the DC-link capacitor is rated at 3.3mF and the voltage is 3000V. However, the actual rated voltage of a single aluminum electrolytic capacitor cannot be achieved, so the rated voltage of the DC link capacitor must be increased by using capacitor banks in series and in parallel. In this paper, a 4×4 serial-to-parallel structure is used in which the capacitance of a single capacitor is rated at 3.3mF and the voltage is 750V.

Assuming that the loss level of each capacitor is equivalent, the capacitor C_1 is used as the test unit. Through the simulation test, the voltage U_{cap} of the C_1 capacitor and the RMS of the current I_{rms} are represented for each system operation.

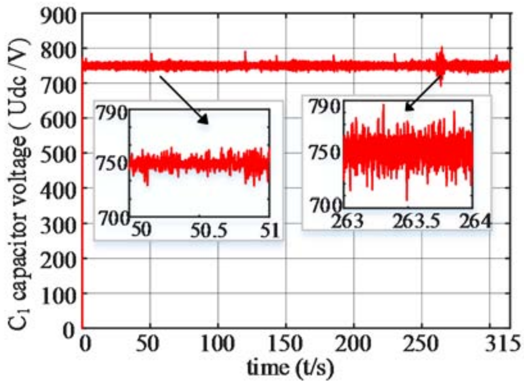

Fig. 3: The simulation result of the capacitor voltage

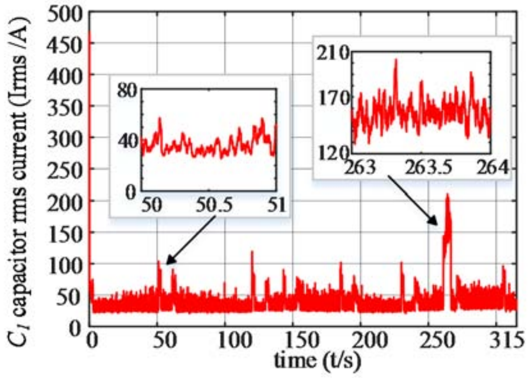

Fig. 4: The simulation result of the capacitor current

The simulation results of U_{cap} and I_{rms} are respectively shown in Fig.3 and Fig.4, which can be seen that the oscillation occurs when executing the variation of the operation conditions, and at different times, under different working conditions, the oscillation degree of voltage and current is also different.

III. Analysis of Capacitor Hot Spot Temperature and Lifetime

A. DFT Analysis Based on Python Toolbox

According to the lifetime model of the capacitor, in order to calculate the hot spot temperature of the DC-link capacitor in the traction drive system operation, the spectrum analysis and accurate calculation of the I_{rms} should be required. The acquired I_{rms} signals are subjected to Discrete Fourier Analysis (DFT) by Python software.

Considering that during operation, the voltage and current of the DC-link capacitor change as the operating conditions change, the DFT analysis needs to select the appropriate grouping:

$$I_{rms}(f)=\begin{bmatrix} H(f_1,h_1) & H(f_2,h_1) & \dots & H(f_i,h_1) \\ H(f_1,h_2) & H(f_2,h_2) & \dots & \dots \\ \dots & \dots & \dots & \dots \\ H(f_1,h_k) & \dots & \dots & H(f_i,h_k) \end{bmatrix}\begin{bmatrix} I_{DC}(h_1) \\ I_{DC}(h_2) \\ \dots \\ I_{DC}(h_k) \end{bmatrix} \quad (3)$$

where $H(f_i, h_k)$ represents the ratio of the harmonic of the I_{rms} of kth group when the frequency is f_i to the K group fundamental wave ($I_{DC}(h_k)$). Among them, K=315 (take a group every minute). At the same time, frequency f_i is taken from 1 to 10kHz(take one at interval 1).

Because of a certain time change of the capacitor current in the short time of system condition changes, only one single packet has a large error. Here, a sliding window method is used, and the grouping module is respectively shifted left and right by n units, totaling $2n+1$ units to find the mean:

$$\begin{cases} H(f_i,h_k)=\dfrac{\sum_{m=-n}^{n} H(f_i,h_{(k,m)})}{2n+1} \\ I_{DC}(h_k)=\dfrac{\sum_{m=-n}^{n} I_{DC}(h_{k,m})}{2n+1} \end{cases} \quad (4)$$

B. Neural Network Fitting of ESR

Consulting the relevant technical manual, the ESR is a complex function of temperature and frequency, and the law of variation is non-linear. The temperature and frequency map to the ESR by using a simple neural network structure, as shown in Fig.5. The input layer is temperature and frequency, and the output layer is the equivalent resistance [13].

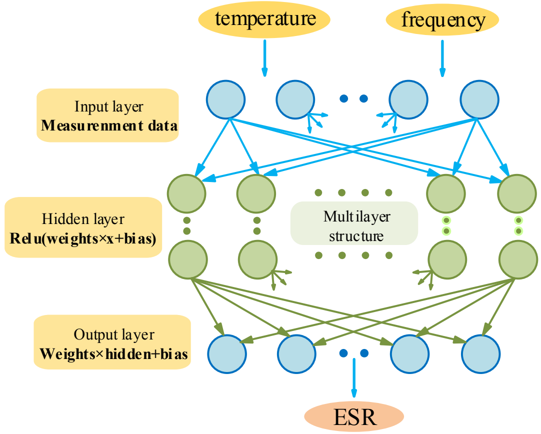

Fig. 5: Neural network structure of the ESR

The neural network is a suitable path toward the solution of the change of frequency and temperature, and based on this, the simulation results of the ESR with different frequency and temperature are shown in Fig.6. The variation law of the ESR is consistent with the technical manual provided by the manufacturer and the conclusion of the ESR test of the aluminum electrolytic capacitor [7].

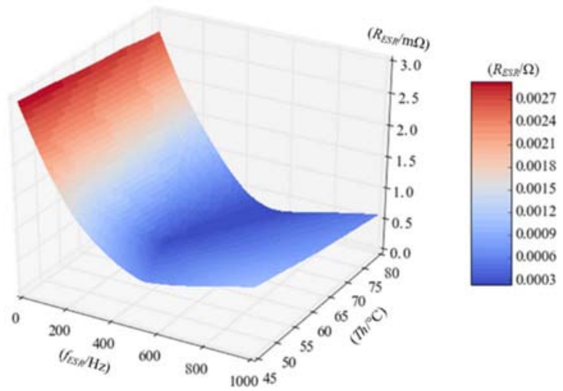

Fig. 6: The fitting result of ESR with different frequency and temperature

C. The Application of Newton's Law of Cooling

However, not only the hot spot temperature is affected by the instantaneous action, but also it is affected by the temperature change within a certain period of time. *Newton's law of cooling* is a suitable path toward the solution of law of device temperature change, and based on this, the optimization model of capacitor hot spot temperature is given as [15]:

$$T_h=(T_1-T_0)\cdot\exp\left\{\left|In(\frac{T_2-T_0}{T_1-T_0})\times\frac{1}{tr}\right|(t-1)\right\}+T_0 \quad (5)$$

where T_2, T_1 and t_r represent the capacitance case temperature of the heat dissipation processes t_2 and t_1 and the time from t_2 to t_1. T_0 represents the final cooling temperature.

A time-temperature trend curve is obtained by performing multiple infrared imaging measurements on the test capacitor cooling process, as shown in Fig.7. This figure shows that the temperature of the capacitor at a certain moment is not only affected by the effect of the moment, but also by the effect of the previous period. The capacitor hot spot temperature is optimized by the influence weights at different times.

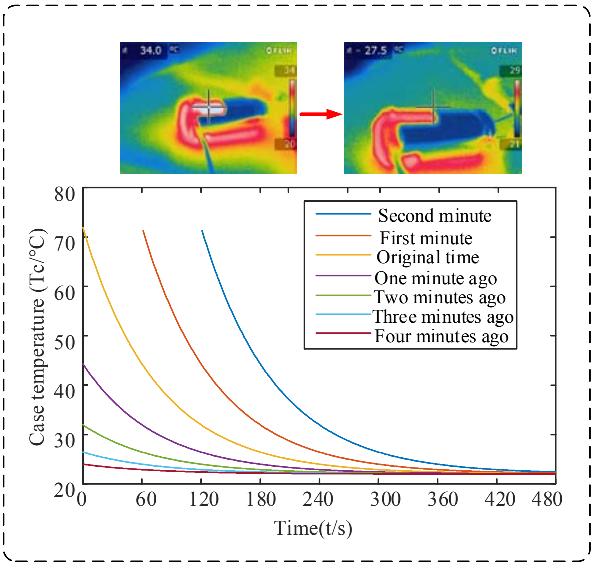

Fig. 7: The results of capacitance heat dissipation

D. Life Model Calculation

The data of the $ESR(f_i)$ and $I_{rms}(f_i)$ are substituted into (2) to obtain a temperature profile. As shown in Fig.8, from top to bottom, this figure represents the original calculated hot spot temperature, the hot spot temperature using Newton's cooling law, and the hot spot temperature using the sliding window.

It can be seen that when the DC-Link capacitor is used in the traction drive system, the hot spot temperature of the capacitor constantly change, and the high temperature point also confirms the influence of the change of working conditions. The introduction of Newton's law of cooling and sliding window method can make the temperature change more stable and closer to the actual operation.

Further, Th, V and manufacturer's rating data are substituted into (1) yielded the lifetime expectancy, as shown in Fig.9.

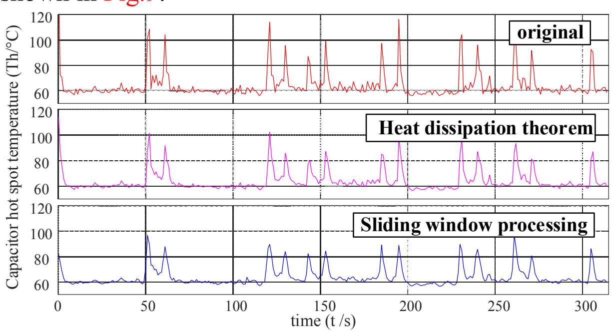

Fig. 8: The simulation result of capacitor hot spot temperature

In order to characterize the overall lifetime of the system in one operation, the further discrete lifetime expectancy values are converted to lifetime loss curves, as shown in Fig.10. The system operates with a capacitance loss of **0.01642%**, so the capacitor can operate **6090.27 times** with an equivalent lifetime of **31973.91 hours**.

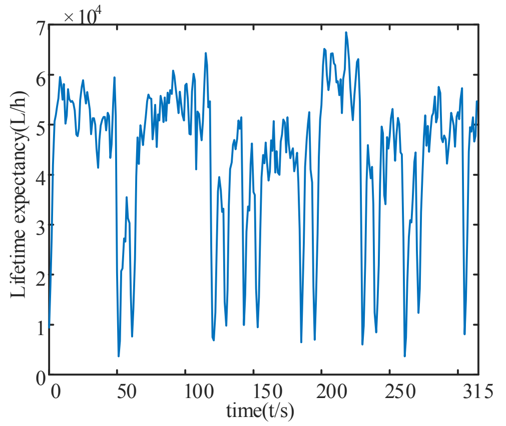

Fig. 9: The simulation result of capacitor lifetime expectancy

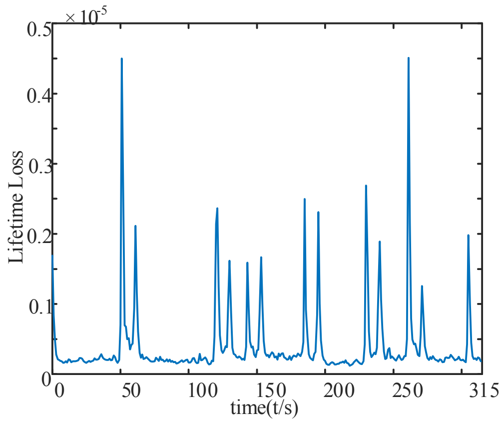

Fig. 10: The simulation result of capacitor lifetime loss

IV. EXPERIMENTAL TEST AND OPTIMIZATION OF CUMULATIVE CAPACITANCE LOSS

During the operation of the system, the capacitor gradually deteriorates. The typical end-of-life criteria of the aluminum electrolytic capacitor is to reduce the capacitance by more than 20% and double the ESR [2].

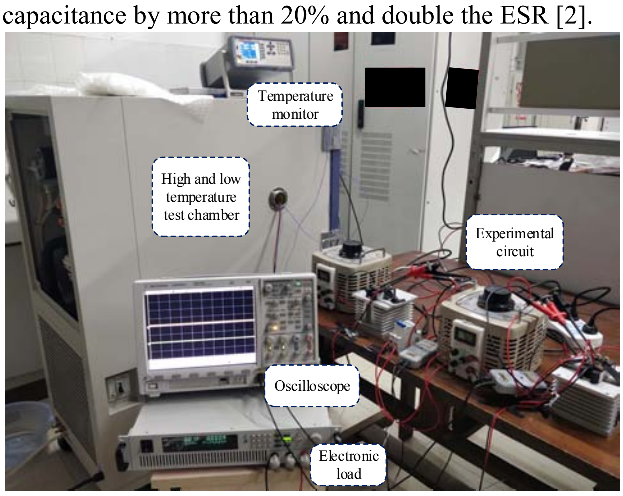

Fig. 11: Experimental test platform

As shown in Fig.11, two sets of accelerated aging experimental platforms for testing the capacitance and equivalent resistance of DC-link capacitors are built. The capacitors have been tested, and the changes of capacitance and equivalent resistance have been statistically analyzed.

The design idea of the accelerated aging experiment is shown in Fig.12. The high and low temperature test chamber is used to set a constant temperature and constant humidity test environment for the capacitor, and the impedance of the load is changed by the programmable electronic load to simulate the change of the actual operating conditions.

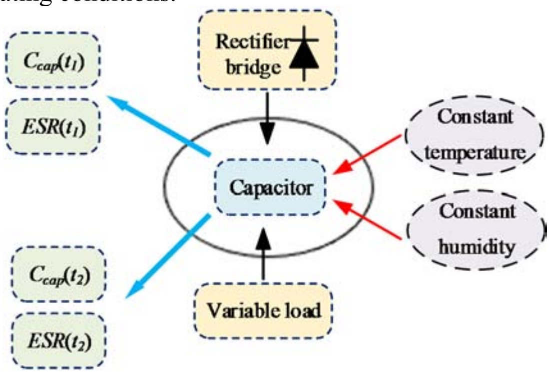

Fig. 12: Experimental design ideas

The C_{cap} and the ESR obtained from the experiment are fitted as shown in Fig.13. The capacitor lifetime estimation under different levels of capacitance loss are shown in Table III.

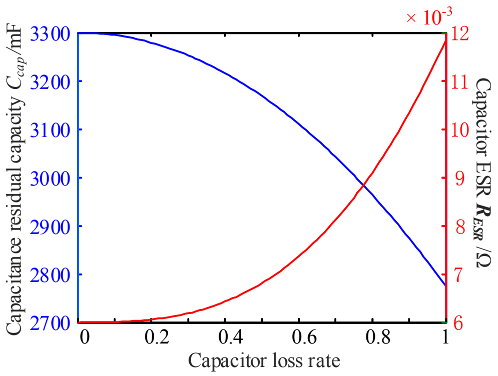

Fig. 13: The experimental result of the capacitance and ESR loss

TABLE III
CAPACITOR LIFETIME ESTIMATION UNDER DIFFERENT LEVELS OF CAPACITANCE LOSS

Damage rate	Orig.	10%	20%	30%	40%
ESR(mΩ)	6	6.014	6.105	6.265	6.592
C_{cap} (uF)	3300	3294	3279	3253	3216
loss ratio(‰)	0.164	0.175	0.162	0.165	0.175
life (/10000h)	3.197	2.996	3.243	3.184	3.001
Damage rate	50%	60%	70%	80%	90%
ESR(mΩ)	7.034	7.632	8.399	9.349	10.5
C_{cap} (uF)	3169	3111	3043	2964	2875
loss ratio(‰)	0.17	0.173	0.174	0.174	1.431
life (/10000h)	3.083	3.033	3.015	3.017	0.367

Due to the robustness of the system, when the capacitance loss rate is within a certain range (0~80%), the life expectancy of the capacitor is basically unchanged. When the capacitance loss rate exceeds 90%, the current and voltage ripple of the capacitor continue to increase due to the multi-operation conditions. As can be seen from Figs.13-15, the capacitor lifetime expectancy drop sharply and the capacitor l lifetime loss rise sharply.

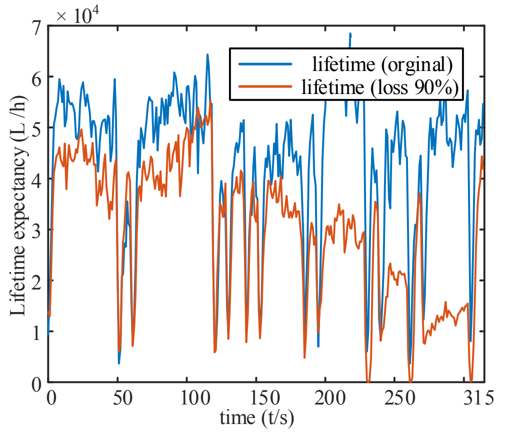

Fig. 13: The lifetime expectancy of the original and 90% loss capacitor

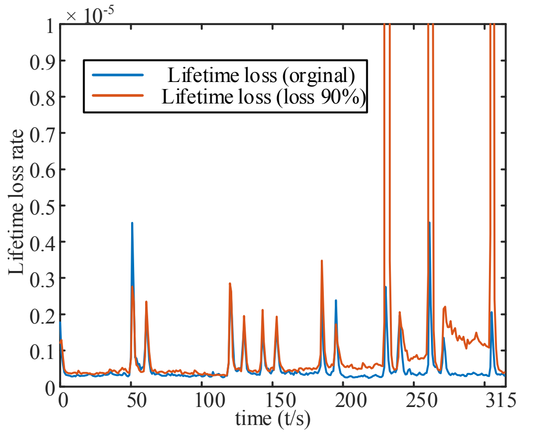

Fig. 14: The lifetime loss of the original and 90% loss capacitor

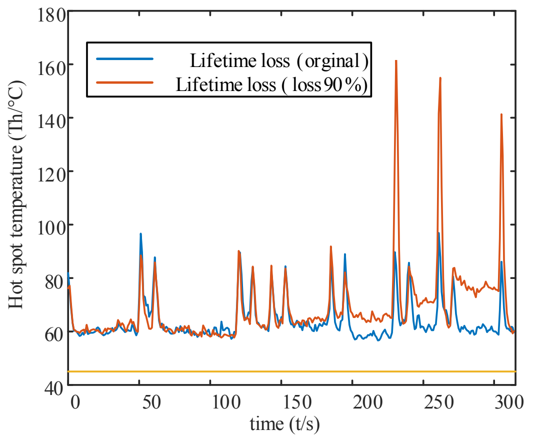

Fig. 15: The hot spot temperature of the original and 90% loss capacitor

Considering the safe operation of the system, the lifetime of unstable operation when the capacitance loss exceeds 90% is removed. Finally, it can be estimated that the life of the capacitor is about **27177.86 hours**, which is equivalent to the life of **8.62 years**, slightly lower than the mandatory replacement period of 12 years. When setting the environmental temperature parameters, this paper takes a higher average. Life expectancy is expected to increase when considering the effects of seasonal changes on ambient temperature. The result can provide a certain reference for the reliability evaluation of the DC-Link capacitor in the traction drive system under complex working conditions.

V. Conclusions

This paper study a method for predicting the life of a capacitor, which can provide accurate life estimation under multi-mode operation. Starting from the capacitor life model, this method converts the actual train conditions into the calculation of traction load. Then the DFT analysis and neural network method are used to solve the capacitor hot spot temperature, and the sliding window and *Newton's law of cooling* are introduced to optimize. Finally, the loss law of capacitance and the ESR is analyzed by accelerated the aging test, and a reasonable lifetime estimation is given considering safe operation.

Acknowledgment

This work was supported by the Research Fund for the National Science Foundation of China (51677156, 61733015).

References

[1] H. Wang, Y. Yang and F. Blaabjerg, "Reliability-oriented design and analysis of input capacitors in single-phase transformer-less photovoltaic inverters," in 2013 *Twenty-Eighth Annual IEEE APEC*, Long Beach, CA, 2013, pp. 2929-2933

[2] H. Wang and F. Blaabjerg, "Reliability of capacitors for DC-link applications in power electronic converters—an overview," *IEEE Trans. Ind. Appl.*, vol. 50, no. 5, pp. 3569-3578, Sept./Oct. 2014.

[3] B. Sun, X. Fan, C. Qian and G. Zhang, "Pof-simulation-assisted reliability prediction for electrolytic capacitor in LED drivers," *IEEE Trans. Ind. Electron.*, vol. 63, no. 11, pp. 6726-6735, Nov. 2016.

[4] H. Wang, P. Davari, H. Wang, D. Kumar, F. Zare and F. Blaabjerg, "Lifetime estimation of DC-link capacitors in adjustable speed drives under grid voltage unbalances," *IEEE Trans. Power Electron*., 2018 (Early Access)

[5] D. Zhou, H. Wang and F. Blaabjerg, "Mission profile based system-level reliability analysis of DC/DC converters for a backup power application," *IEEE Trans. Power Electron.*, vol. 33, no. 9, pp. 8030-8039, Sept. 2018.

[6] D. Zhou, H. Wang, H. Wang and F. Blaabjerg, "Reliability analysis of grid-interfaced filter capacitors," in *Chinese Journal of Electrical Engineering*, vol. 4, no. 3, pp. 21-28, Sep. 2018.

[7] K. Urata and T. Shimizu, "Temperature estimation of aluminum electrolytic capacitor under actual circuit operation," *2018 International Power Electronics Conference (IPEC-Niigata 2018 -ECCE Asia)*, Niigata, 2018, pp. 302-308.

[8] Y. Yang, K. Ma, H. Wang and F. Blaabjerg, "Instantaneous thermal modeling of the DC-link capacitor in photovoltaic systems," *2015 IEEE Applied Power Electronics Conference and Exposition (APEC)*, Charlotte, NC, 2015, pp. 2733-2739.

[9] Y. Yang, K. Ma, H. Wang and F. Blaabjerg, "Instantaneous thermal modeling of the DC-link capacitor in PhotoVoltaic systems," *2015 IEEE Applied Power Electronics Conference and Exposition (APEC)*, Charlotte, NC, 2015, pp. 2733-2739.

[10] J. Rajmond and P. Dan, "Thermal modeling of through hole capacitors," *2012 IEEE 18th International Symposium for Design and Technology in Electronic Packaging (SIITME)*, Alba Iulia, 2012, pp. 227-232.

[11] M. L. Gasperi and N. Gollhardt, "Heat transfer model for capacitor banks," *Conference Record of 1998 IEEE Industry Applications Conference. Thirty-Third IAS Annual Meeting (Cat. No.98CH36242)*, St. Louis, MO, USA, 1998, pp. 1199-1204 vol.2.

[12] Wang H, Wang H. An analytical circuit based nonlinear thermal model for capacitor banks. *Microelectronics Reliability*, vol. 88, pp. 524-527, Jun. 2018.

[13] H. Wang and H. Wang, "Capacitive DC links in power electronic systems-reliability and circuit design," in *Chinese Journal of Electrical Engineering*, vol. 4, no. 3, pp. 29-36, Sep. 2018.

[14] Y. LeCun, Y. Bengio, and G. Hinton, "Deep learning, " *Nature*, vol.521, no. 7553, pp. 436–444, May 2015.

[15] B. Lee, S. Hyun, H. Lee, S. Shin, C. Won and T. Lee, "Convenient thermal modeling for loss distribution of 3-level Active NPC using newton's law," *2014 IEEE International Conference on Industrial Technology (ICIT)*, Busan, 2014, pp. 409-413.